JOURNAL OF GUIDANCE, CONTROL, AND DYNAMICS
Vol. 28, No. 1, January–February 2005

Engineering Notes

ENGINEERING NOTES are short manuscripts describing new developments or important results of a preliminary nature. These Notes cannot exceed 6 manuscript pages and 3 figures; a page of text may be substituted for a figure and vice versa. After informal review by the editors, they may be published within a few months of the date of receipt. Style requirements are the same as for regular contributions (see inside back cover).

Optimal Three-Dimensional Interplanetary Rendezvous Using Nonideal Solar Sail

Giovanni Mengali* and Alessandro A. Quarta†
University of Pisa, I-56122 Pisa, Italy

Introduction

THE problem of trajectory optimization for solar-sail spacecraft with an ideal force model has been frequently addressed in the literature. Zhukov and Lebedev[1] used the calculus of variations to find optimal solar-sail trajectories for circular, coplanar orbits. Using the same approach, the results have been generalized by Sauer,[2] including inclined, elliptic orbits for the launch and target planets. Other contributions are given by Wood et al.,[3] Subba Rao and Ramanan,[4] and Simon and Zakharov.[5] Each of the preceding papers assumes a perfectly reflecting solar sail and a corresponding thrust force that is normal to the sail surface. Nonideal sails have been seldom considered. Some results have been marginally presented by Sauer[6] during a study for a Halley's comet rendezvous mission. Cichan and Melton[7] studied optimal nonideal solar-sail trajectories including the effects of imperfect reflectivity and sail billowing. In their work, a direct optimization method is used to solve the problem, and only circular and coplanar orbits are investigated. Very recently, Colasurdo and Casalino[8] proposed an indirect approach to minimize the trip time of interplanetary missions. However, their analysis is confined to a bidimensional problem, and a flat sail with a simplified optical model is considered. Also, circular orbits are assumed for the planets.

In this Note an optical and a parametric solar-sail force model are investigated. The force exerted on a nonperfect solar sail is modeled considering reflection, absorption, and reradiation by the sail. Also, the billowing of the sail under load is taken into account. A three-dimensional problem is studied with elliptical and not coplanar orbits. The analysis presented here follows that by Sauer,[2] who considered ideal sails, and the results are extended to the nonideal case. A solution to the optimal control law is found using the calculus of variations and a link between the control laws and the main parameters that define the sail film optical properties, and the sail shape is established.

Received 16 February 2004; revision received 27 May 2004; accepted for publication 8 June 2004.

*Associate Professor, Department of Aerospace Engineering; g.mengali@ing.unipi.it.

†Ph.D. Candidate, Department of Aerospace Engineering; a.quarta@ing.unipi.it.

Equations of Motion

The equations of motion for a spacecraft in a heliocentric inertial frame $\mathcal{T}_\odot(x, y, z)$ are

$$\dot{\boldsymbol{r}} = \boldsymbol{v} \tag{1}$$

$$\dot{\boldsymbol{v}} = -\left(\mu_\odot / r^3\right)\boldsymbol{r} + \boldsymbol{a} \tag{2}$$

where $[\boldsymbol{r}]_{\mathcal{T}_\odot} = [r_x, r_y, r_z]^T$ and $[\boldsymbol{v}]_{\mathcal{T}_\odot} = [v_x, v_y, v_z]^T$ are the spacecraft position and velocity relative to $\mathcal{T}_\odot$ and $\boldsymbol{a}$ is the acceleration caused by the solar radiation pressure. Let $\mathcal{T}_{\text{orb}}(x_{\text{orb}}, y_{\text{orb}}, z_{\text{orb}})$ be an orbital frame whose unit vectors are $\hat{\boldsymbol{i}}_{\text{orb}} \equiv \hat{\boldsymbol{r}}, \hat{\boldsymbol{j}}_{\text{orb}}$ and $\hat{\boldsymbol{k}}_{\text{orb}}$, where $\hat{\boldsymbol{r}} \triangleq \boldsymbol{r}/r$ is the unit vector in the direction of the incident radiation from the sun. Assume that the plane $z_{\text{orb}} = 0$ contains the axis z of the $\mathcal{T}_\odot$ frame and y_{orb} points towards the ecliptic pole. In Fig. 1, $\hat{\boldsymbol{n}}$ is the unit vector normal to the sail in the direction of thrust, $\alpha \in [0, \pi/2]$ is the sail cone angle, and $\delta \in [-\pi, \pi]$ is the sail clock angle, which is positive in the counterclockwise direction. Different models are available to quantify the acceleration $\boldsymbol{a}$ of the solar sail. In the following we distinguish[9] between optical (subscript o) and parametric (subscript p) models.

Optical-Force Model

Let s be the fraction of photons that are specularly reflected by the sail, B_{fr} and B_b are the non-Lambertian coefficients of the front and back sail surfaces, ϵ_{fr} and ϵ_b the corresponding front and back emissivities, and $\rho < 1$ the reflection coefficient. The acceleration $\boldsymbol{a}_o$ of the solar sail can be written as[9]

$$\boldsymbol{a}_o = (\beta/2)\left(\mu_\odot / r^2\right)\left[b_1 \cos\alpha_o\, \hat{\boldsymbol{r}} + \left(b_2 \cos^2\alpha_o + b_3 \cos\alpha_o\right)\hat{\boldsymbol{n}}_o\right] \tag{3}$$

where β is the solar-sail lightness number and

$$b_1 \triangleq 1 - \rho s, \qquad b_2 \triangleq 2\rho s \tag{4}$$

$$b_3 \triangleq B_{\text{fr}}\,\rho(1 - s) + (1 - \rho)\frac{\epsilon_{\text{fr}} B_{\text{fr}} - \epsilon_b B_b}{\epsilon_{\text{fr}} + \epsilon_b} \tag{5}$$

The components of the control vector $\boldsymbol{u}_o$ are

$$[\boldsymbol{u}_o]_{\mathcal{T}_{\text{orb}}} = [\alpha_o, \delta_o]^T \tag{6}$$

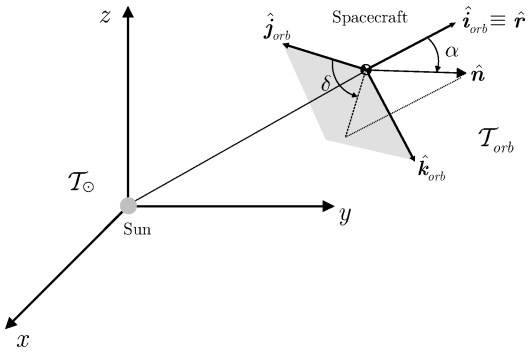

Fig. 1 Reference frames.

Parametric-Force Model

This exact force model is obtained by calculating the sail shape and numerically integrating the radiation pressure across the billowed sail.[9] The modulus of the force $f_p = \|\boldsymbol{f}_p\|$ is parameterized as a function of the force cone angle θ_p between the incoming radiation and the direction of the force unit vector, that is,

$$\cos\theta_p \triangleq \hat{\boldsymbol{r}} \cdot \hat{\boldsymbol{f}}_p \tag{7}$$

The following model for the acceleration is assumed:

$$\boldsymbol{a}_p = (\beta/2)\left(\mu_\odot/r^2\right)(b_1 + b_2 + b_3)\left(c_1\cos^4\theta_p + c_2\cos^2\theta_p + c_3\right)\hat{\boldsymbol{f}}_p \tag{8}$$

where $\theta_p \in [0, \theta_p^*]$, b_1, b_2, b_3 are given by Eqs. (4) and (5); c_1, c_2, c_3 are the parametric force coefficients; and θ_p^* is value of θ_p that makes the modulus of $\boldsymbol{a}_p$ equal to zero, that is,

$$\cos\theta_p^* = \sqrt{\frac{-c_2 + \sqrt{c_2^2 - 4c_1c_3}}{2c_1}} \tag{9}$$

Note that Eq. (8) is equivalent to the model presented in Ref. 9, but a different definition of coefficients c_i has been adopted in order to obtain a compact expression for θ_p^*. Also, the components of the control vector $\boldsymbol{u}_p$ are

$$[\boldsymbol{u}_p]_{\mathcal{T}_{\text{orb}}} = [\theta_p, \delta_p]^T \tag{10}$$

Optimal Control Law

The problem is to find the optimal control law $\boldsymbol{u}(t)$ (where $t \in [0, t_f]$), which minimizes the time t_f necessary to transfer the spacecraft from an initial $(\boldsymbol{r}_0, \boldsymbol{v}_0)$ to a final $(\boldsymbol{r}_f, \boldsymbol{v}_f)$ prescribed state. This amounts to maximizing the performance index:

$$J = -t_f \tag{11}$$

From Eqs. (1) and (2) the Hamiltonian of the system is

$$H = \boldsymbol{\lambda}_r \cdot \boldsymbol{v} - \left(\mu_\odot/r^3\right)\boldsymbol{\lambda}_v \cdot \boldsymbol{r} + \boldsymbol{\lambda}_v \cdot \boldsymbol{a} \tag{12}$$

where $\boldsymbol{\lambda}_r \triangleq [\lambda_{r_x}, \lambda_{r_y}, \lambda_{r_z}]^T$ and $\boldsymbol{\lambda}_v \triangleq [\lambda_{v_x}, \lambda_{v_y}, \lambda_{v_z}]^T$ are the vectors adjoint to the position and the velocity, respectively. Recall that $\boldsymbol{\lambda}_v$ is referred to as the primer vector.[10] The orientation of $\boldsymbol{\lambda}_v$ is defined through the primer vector cone angle $\tilde{\theta} \in [0, \pi]$ and clock angle $\tilde{\delta} \in [-\pi, \pi]$.

In this Note the boundary conditions are constrained by the planetary ephemerides.[11] Accordingly,

$$\boldsymbol{r}_f = \boldsymbol{r}^{(p)}(t_f), \qquad \boldsymbol{v}_f = \boldsymbol{v}^{(p)}(t_f) \tag{13}$$

where $\boldsymbol{r}^{(p)}$ and $\boldsymbol{v}^{(p)}$ are the position and velocity of the target planet. Observing that $\dot{\boldsymbol{r}}^{(p)}(t_f) = \boldsymbol{v}_f$ and $\dot{\boldsymbol{v}}^{(p)}(t_f) = -\mu_\odot \boldsymbol{r}_f/r_f^3$, the transversality condition is given by[2,12]

$$H(t_f) = 1 + \boldsymbol{\lambda}_r(t_f) \cdot \boldsymbol{v}_f - \left(\mu_\odot/r_f^3\right)\boldsymbol{\lambda}_v(t_f) \cdot \boldsymbol{r}_f \tag{14}$$

From the Pontryagin's maximum principle the optimal control law $\boldsymbol{u}(t)$, to be selected in the domain of feasible controls $\mathcal{U}$, is such that, at any time, the Hamiltonian is an absolute maximum. This amounts to maximizing the function H', which coincides with that portion of the Hamiltonian H that explicitly depends on the control vector, that is,

$$\boldsymbol{u} = \arg\max_{u \in \mathcal{U}} H \equiv \arg\max_{u \in \mathcal{U}} H' \qquad \text{with} \qquad H' \triangleq \boldsymbol{\lambda}_v \cdot \boldsymbol{a} \tag{15}$$

Optical-Force Model

Substituting the acceleration equation (3) into Eq. (12), the Hamiltonian becomes

$$H_o = \boldsymbol{\lambda}_{r_o} \cdot \boldsymbol{v} - \left(\mu_\odot/r^3\right)\boldsymbol{\lambda}_{v_o} \cdot \boldsymbol{r} + \left(\beta\mu_\odot/2r^2\right)\left[b_1\cos\alpha_o\left(\boldsymbol{\lambda}_{v_o} \cdot \hat{\boldsymbol{r}}\right) + \left(b_2\cos^2\alpha_o + b_3\cos\alpha_o\right)\left(\boldsymbol{\lambda}_{v_o} \cdot \hat{\boldsymbol{n}}_o\right)\right] \tag{16}$$

and the Euler–Lagrange equations are

$$\dot{\boldsymbol{\lambda}}_{r_o} = \left(\mu_\odot/r^3\right)\boldsymbol{\lambda}_{v_o} - \left(3\mu_\odot/r^5\right)\left(\boldsymbol{\lambda}_{v_o} \cdot \boldsymbol{r}\right)\boldsymbol{r} + (2\boldsymbol{r}/r^2)\left(\boldsymbol{a}_o \cdot \boldsymbol{\lambda}_{v_o}\right) - \left(\beta\mu_\odot/2r^2\right)\left[b_1\boldsymbol{d}_1\left(\hat{\boldsymbol{r}} \cdot \boldsymbol{\lambda}_{v_o}\right) + b_1\cos\alpha_o\,\boldsymbol{d}_2 + \boldsymbol{d}_1\left(\hat{\boldsymbol{n}}_o \cdot \boldsymbol{\lambda}_{v_o}\right)(2b_2\cos\alpha_o + b_3)\right] \tag{17}$$

$$\dot{\boldsymbol{\lambda}}_{v_o} = -\boldsymbol{\lambda}_{r_o} \tag{18}$$

where

$$\boldsymbol{d}_1 \triangleq (1/r)[\hat{\boldsymbol{n}}_o - (\hat{\boldsymbol{r}} \cdot \hat{\boldsymbol{n}}_o)\hat{\boldsymbol{r}}], \qquad \boldsymbol{d}_2 \triangleq (1/r)\left[\boldsymbol{\lambda}_{v_o} - \left(\hat{\boldsymbol{r}} \cdot \boldsymbol{\lambda}_{v_o}\right)\hat{\boldsymbol{r}}\right] \tag{19}$$

The optimal control law is found by maximizing the function

$$H_o' = \left(\beta\mu_\odot/2r^2\right)\left[b_1\cos\alpha_o\left(\boldsymbol{\lambda}_{v_o} \cdot \hat{\boldsymbol{r}}\right) + \left(b_2\cos^2\alpha_o + b_3\cos\alpha_o\right)\left(\boldsymbol{\lambda}_{v_o} \cdot \hat{\boldsymbol{n}}_o\right)\right] \tag{20}$$

Letting $\partial H_o'/\partial \boldsymbol{u}_o = 0$, provides

$$\tan\tilde{\theta}_o = \frac{\sin\alpha_o\left(b_1 + 3b_2\cos^2\alpha_o + 2b_3\cos\alpha_o\right)}{\cos^2\alpha_o(b_2\cos\alpha_o + b_3) - \sin^2\alpha_o(2b_2\cos\alpha_o + b_3)} \tag{21}$$

$$\tan\delta_o = \tan\tilde{\delta}_o \tag{22}$$

Note, however, that a generic point $(\alpha_o, \tilde{\theta}_o)$ solution of Eq. (21) is a maximum for H_o' provided that $H_o'(\alpha_o, \tilde{\theta}_o) \geq 0$. It can be verified that

$$H_o' \geq 0 \Leftrightarrow \tan\tilde{\theta}_o \leq -\frac{b_1 + \cos\alpha_o(b_2\cos\alpha_o + b_3)}{\sin\alpha_o(b_2\cos\alpha_o + b_3)} \tag{23}$$

Consider the following two functions $f_1(\alpha_o)$ and $f_2(\alpha_o)$:

$$\tilde{\theta}_{o_1} = f_1(\alpha_o): \qquad H_o'(\alpha_o, f_1(\alpha_o)) = 0 \tag{24}$$

$$\tilde{\theta}_{o_2} = f_2(\alpha_o): \qquad \partial H_o'(\alpha_o, f_2(\alpha_o))/\partial\alpha_o = 0 \tag{25}$$

Substituting Eq. (23) (taken with the equal sign) into Eq. (21) provides the values of $\alpha_o = \alpha_o^*$ such that $f_1 = f_2$. It turns out that the unique solution in the range $\alpha_o \in [0, \pi/2)$ is given by the critical cone angle α_o^*:

$$\cos\alpha_o^* = \frac{-b_1b_3 - 2b_2b_3 + \sqrt{b_1^2b_3^2 - 4b_1b_3^2b_2 + 8b_1^2b_2^2 + 4b_2^3b_1}}{4b_1b_2 + 2b_2^2} \tag{26}$$

As long as $\alpha_o \in [0, \alpha_o^*)$, it happens that $f_2 < f_1$, whereas when $\alpha_o \in (\alpha_o^*, \pi/2)$, then $f_2 > f_1$. This situation is illustrated in Fig. 2 for a Jet Propulsion Laboratory (JPL) square sail ($\alpha_o^* \cong 72.6$ deg) whose data have been derived from the Halley's comet rendezvous study.[13,14]

To summarize, Eq. (21) gives the optimal sail cone angle α_o as a function of $\tilde{\theta}_o$ and of the sail parameters b_1, b_2, and b_3, provided that α_o is in the interval $[0, \alpha_o^*]$. Otherwise, the optimal sail cone angle is $\alpha_o = \pi/2$, that is, when the sail produces no thrust [see Eq. (3)] and H_o' is zero. This implies that coast arcs can appear in the optimal trajectory of a nonideal solar sail, in accordance with the same result that was first obtained by Sauer.[6] As a consequence of Eq. (22), the unit vectors $\hat{\boldsymbol{n}}_o$, $\hat{\boldsymbol{r}}$, and $\hat{\boldsymbol{\lambda}}_{v_o} \triangleq \boldsymbol{\lambda}_{v_o}/\lambda_{v_o}$ are coplanar. This allows one to remove the dependence on $\hat{\boldsymbol{n}}_o$ in the equations of motion [see Eqs. (2) and (3)] and in the Euler–Lagrange equations. The result is

$$\hat{\boldsymbol{n}}_o = \begin{cases} \dfrac{\sin(\tilde{\theta}_o - \alpha_o)}{\sin\tilde{\theta}_o}\hat{\boldsymbol{r}} + \dfrac{\sin\alpha_o}{\sin\tilde{\theta}_o}\hat{\boldsymbol{\lambda}}_{v_o} & \text{for} \quad \tilde{\theta}_o \in (0, \pi) \\ \hat{\boldsymbol{r}} & \text{for} \quad \tilde{\theta}_o = 0 \end{cases} \tag{27}$$

where

$$\cos\theta_o = \hat{\boldsymbol{\lambda}}_{v_o} \cdot \hat{\boldsymbol{r}}, \qquad \sin\tilde{\theta}_o = \left|\hat{\boldsymbol{\lambda}}_{v_o} \times \hat{\boldsymbol{r}}\right| \tag{28}$$

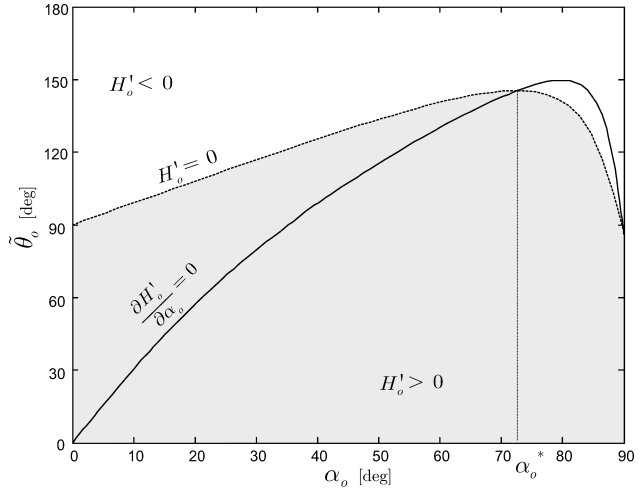

Fig. 2 Optimum sail cone angle α_o for JPL square sail with optical force model.

Observe that $\tilde{\theta}_o = \pi$ corresponds to $\alpha_o = \pi/2$ [see Eq. (21) and Fig. 2]. Correspondingly, all of the terms containing $\hat{\boldsymbol{n}}_o$ vanish both in the equations of motion (because $\boldsymbol{a}_o \equiv 0$) and in the Euler–Lagrange equations. As a consequence of Eqs. (27) and (3), the optimal control law requires the thrust vector to lie in the plane defined by the position vector $\boldsymbol{r}$ and the primer vector $\boldsymbol{\lambda}_v$. This generalizes the same result found by Sauer for an ideal sail.[2]

Parametric-Force Model

Substituting the acceleration equation (8) into Eq. (12), the Hamiltonian becomes

$$H_p = \boldsymbol{\lambda}_{r_p} \cdot \boldsymbol{v} - \left(\mu_\odot / r^3\right)\boldsymbol{\lambda}_{v_p} \cdot \boldsymbol{r} + (\beta/2)\left(\mu_\odot / r^2\right)(b_1 + b_2 + b_3) \times \left(c_1 \cos^4\theta_p + c_2 \cos^2\theta_p + c_3\right)\left(\boldsymbol{\lambda}_{v_p} \cdot \hat{f}_p\right) \tag{29}$$

and the Euler–Lagrange equations are

$$\dot{\boldsymbol{\lambda}}_{r_p} = \left(\mu_\odot / r^3\right)\boldsymbol{\lambda}_{v_p} - \left(3\mu_\odot / r^5\right)\left(\boldsymbol{\lambda}_{v_p} \cdot \boldsymbol{r}\right)\boldsymbol{r} + 2\left(\boldsymbol{a}_p \cdot \boldsymbol{\lambda}_{v_p}\right)(\hat{\boldsymbol{r}}/r) - \left[\cos\theta_p \beta\mu_\odot (b_1 + b_2 + b_3)\left(2c_1 \cos^2\theta_p + c_2\right)\left(\hat{\boldsymbol{f}}_p \cdot \boldsymbol{\lambda}_{v_p}\right) \times \left(\hat{\boldsymbol{f}}_p - \cos\theta_p \hat{\boldsymbol{r}}\right)/r^3\right] \tag{30}$$

$$\dot{\boldsymbol{\lambda}}_{v_p} = -\boldsymbol{\lambda}_{r_p} \tag{31}$$

The function to be maximized is

$$H_p' = \frac{\beta(b_1 + b_2 + b_3)\mu_\odot}{2r^2}\left(c_1 \cos^4\theta_p + c_2 \cos^2\theta_p + c_3\right)\left(\hat{\boldsymbol{f}}_P \cdot \boldsymbol{\lambda}_{v_p}\right) \tag{32}$$

Letting $\partial H_p'/\partial \boldsymbol{u}_p = 0$, yields

$$\tan(\tilde{\theta}_p - \theta_p) = \frac{2\sin\theta_p \cos\theta_p \left(2c_1 \cos^2\theta_p + c_2\right)}{c_1 \cos^4\theta_p + c_2 \cos^2\theta_p + c_3} \tag{33}$$

$$\tan\delta_p = \tan\tilde{\delta}_p \tag{34}$$

In this case it is found that

$$H_p' \geq 0 \Leftrightarrow \tilde{\theta}_p \leq \theta_p + \pi/2 \tag{35}$$

Consider the following two functions $f_1(\theta_p)$ and $f_2(\theta_p)$:

$$\tilde{\theta}_{p_1} = f_1(\theta_p): \qquad H_o'(\theta_p, f_1(\theta_p)) = 0 \tag{36}$$

$$\tilde{\theta}_{p_2} = f_2(\theta_p): \qquad \partial H_o'(\theta_p, f_2(\theta_p))/\partial\theta_p = 0 \tag{37}$$

Substituting Eq. (35) (taken with the equal sign) into Eq. (33) provides the values of θ_p such that $f_1 = f_2$. It turns out that the unique solution in the range $\theta_p \in [0, \theta_p^*]$ is $\theta_p = \theta_p^*$, where θ_p^* is exactly the critical cone angle that makes the solar-sail thrust equal to zero and whose value is given by Eq. (9). Correspondingly one has

$$\tilde{\theta}_p^* = \theta_p^* + \pi/2 \tag{38}$$

In other terms, as long as $\theta_p \in [0, \theta_p^*)$ it happens that $f_2 < f_1$, as is shown in Fig. 3 for a JPL square sail ($\theta_p^* \cong 61$ deg).

To summarize, Eq. (33) gives the optimal sail cone angle θ_p as a function of $\tilde{\theta}_p$ and of the sail parameters c_1, c_2, and c_3, provided that θ_p is in the interval $[0, \theta_p^*]$. Otherwise, the optimal force cone angle is $\theta_p = \theta_p^*$. Once more, coast arcs can appear in the optimal trajectory of a parametric solar-sail model.

Finally, observing that the unit vectors $\hat{\boldsymbol{r}}$, $\hat{\boldsymbol{f}}_P$, and $\hat{\boldsymbol{\lambda}}_{v_p} \triangleq \boldsymbol{\lambda}_{v_p}/\lambda_{v_p}$ are coplanar [see Eq. (34)], the dependence on $\hat{\boldsymbol{f}}_p$ in the equations of

Table 1 Optical and force coefficients for a JPL square sail (derived from Ref. 9)

Coefficient	Value
b_1	0.1728
b_2	1.6544
b_3	−0.0109
c_1	−0.088
c_2	1.412
c_3	−0.324

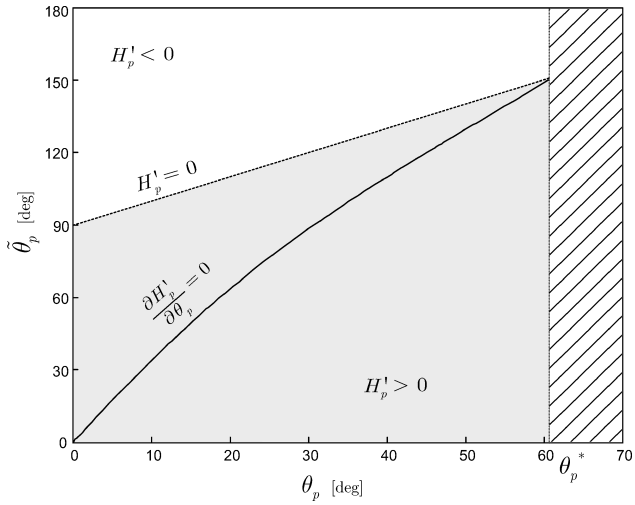

Fig. 3 Optimum force cone angle θ_p for JPL square sail with parametric force model.

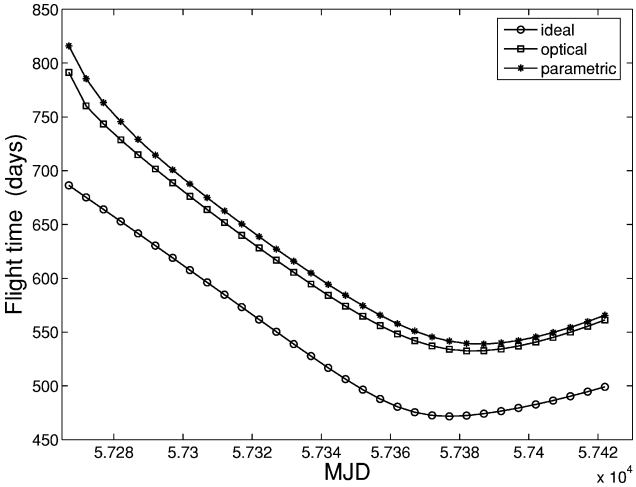

Fig. 4 Flight times for a Mars mission with different sail force models. The control law for the ideal sail is taken from Sauer.[2]

motion and in the Euler–Lagrange equations can be removed. In fact,

$$\hat{\boldsymbol{f}}_p = \begin{cases} \dfrac{\sin(\tilde{\theta}_p - \theta_p)}{\sin\tilde{\theta}_p}\hat{\boldsymbol{r}} + \dfrac{\sin\theta_p}{\sin\tilde{\theta}_p}\hat{\boldsymbol{\lambda}}_{v_p} & \text{for} \quad \tilde{\theta}_p \in \left(0, \tilde{\theta}_p^*\right) \\ \hat{\boldsymbol{r}} & \text{for} \quad \tilde{\theta}_p = 0 \end{cases} \tag{39}$$

where $\cos\tilde{\theta}_p$ and $\sin\tilde{\theta}_p$ are calculated from Eq. (28) by substituting $\tilde{\theta}_o$ and $\hat{\boldsymbol{\lambda}}_{v_o}$ with $\tilde{\theta}_p$ and $\hat{\boldsymbol{\lambda}}_{v_p}$, respectively. Also, the direction of the unit vector $\hat{\boldsymbol{f}}_p$ should not be calculated for $\tilde{\theta}_p \geq \tilde{\theta}_p^*$ because, in that case, $\theta_p = \theta_p^*$ and the sail produces no thrust. Note that, as in the case of optical force model, the thrust vector is required to lie in the plane defined by the position vector $\boldsymbol{r}$ and the primer vector $\boldsymbol{\lambda}_v$.

Case Study

The control laws described earlier have been applied to study the heliocentric phase of a three-dimensional Mars mission of a solar sail with optical and parametric models. The coefficients b_i and c_i are relative to a JPL square sail (Table 1). Both positions and velocities of the planets at departure and arrival are calculated by means of ephemeris data. The trajectories are characterized by zero values of hyperbolic excess speed at both endpoints. A value of solar-sail lightness number $\beta = 0.1175$ is assumed. (The corresponding value of the characteristic accelerations in the ideal case is 0.7 mm/s^2.) A set of canonical units[15] has been used in the integration of the differential equations to reduce their numerical sensitivity. The differential equations have been integrated in double precision using a Runge–Kutta fifth-order scheme with absolute and relative errors of 10^{-12}. The boundary-value problem associated to the variational problem has been solved by means of a hybrid numerical technique that combines the use of genetic algorithms[16] to obtain a rough estimate of the adjoint variables, with gradient-based and direct methods[17,18] to refine the solution. This technique allows one to reach the solution with virtually no need of trial-and-error procedures. A number of trajectories have been investigated in the time

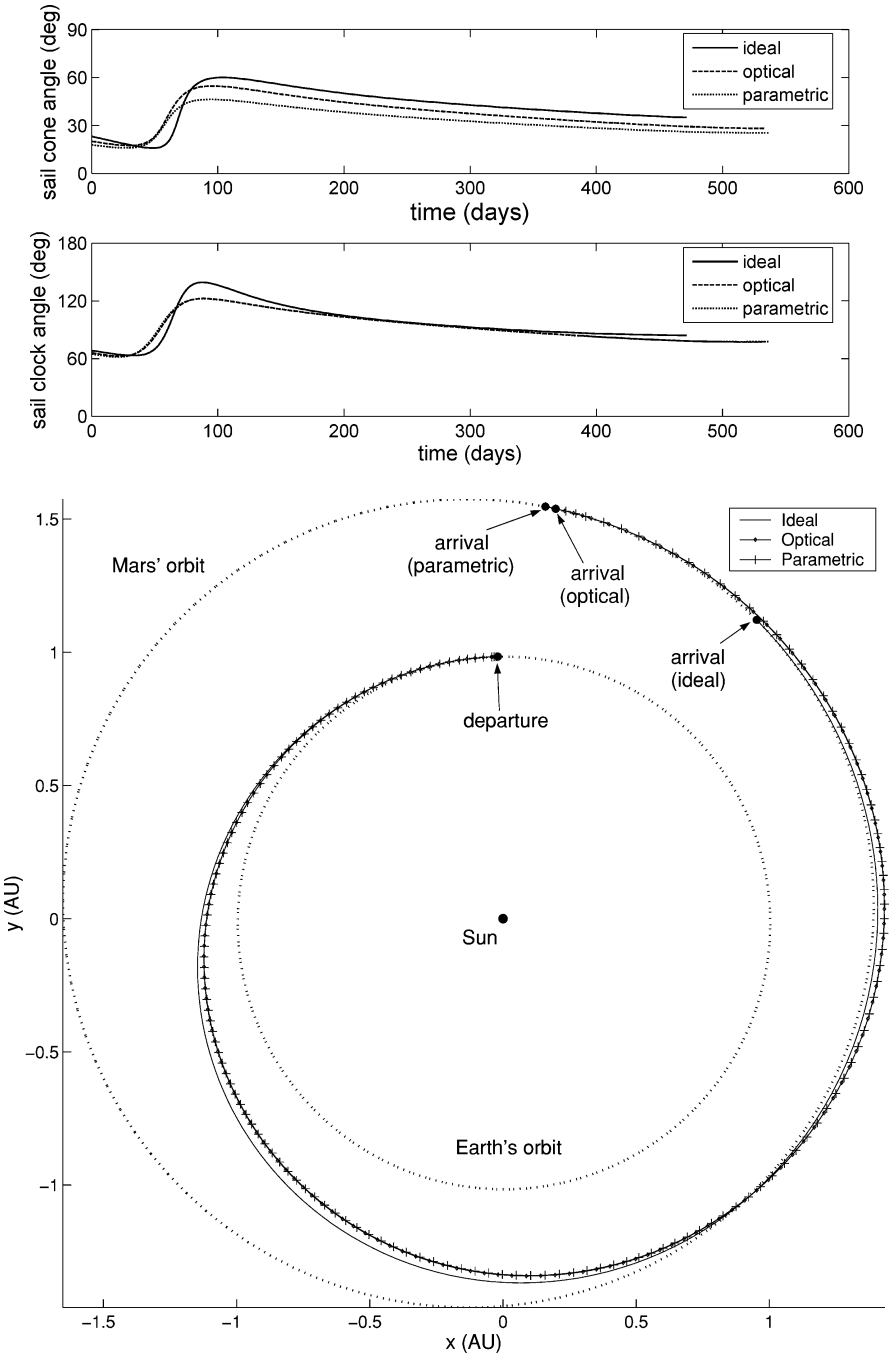

Fig. 5 Control angles and projection on the ecliptic plane of the solar-sail Mars trajectories (starting date 21 December 2015).

interval ranging from September 2015 to February 2016. In all of the simulations performed, the endpoint constraints are satisfied to better than 10^{-10}. A comparison of mission times as a function of the modified Julian date is shown in Fig. 4. Simulations reveal that nonideal sails require a considerable increase of flight time (when compared to an ideal sail), on the order of 12–13% for an optical model and 14–15% for a parametric model. These results are in agreement with Dachwald,[19] who investigated optimal trajectories for nonideal solar sail using evolutionary neurocontrol. The minimum transfer time (470 days) for an ideal sail is in excellent agreement with the results reported by Sauer.[2] Note that the minimum transfer times for the optical and parametric models (equal to 532 and 539 days, respectively) are obtained with starting dates close to the optimal launch date for the ideal case (21 December 2015). The corresponding time histories of control angles and trajectories are shown in Fig. 5. Note that the control laws satisfy the constraints $\alpha_o \leq \alpha_o^*$ and $\theta_p \leq \theta_p^*$ defined by Eqs. (26) and (9) (see also Figs. 2 and 3). Simulations with coast arcs, not shown here for space limitations, have been found in some trajectories of a nonideal solar sail. Both the transfer time and the time histories of control angles illustrated in Fig. 5 are similar to the values obtained by Colasurdo and Casalino[8] under the assumption of circular and coplanar planet orbits.

Conclusions

Minimum time trajectories of nonideal solar sail for interplanetary missions have been investigated using an indirect approach. The real shape and space orientation of both the departure and arrival planetary orbits are considered. Optical- and parametric-force models have been investigated, where the force exerted on a nonperfect solar sail is applied, considering reflection, absorption, and reradiation by the sail. Also, the billowing of the sail under load has been taken into account. Using the theory of variational calculus, the analytical expressions of the control laws that define the optimal orientation of the sail are found. Accordingly, a link is established between the variation intervals of the control angles and the physical parameters that define the sail behavior under the action of the solar radiation pressure. In particular, the optimal steering law for both optical and parametric models requires the thrust vector to lie in the plane defined by the position vector and the primer vector. This conclusion extends a similar result found by Sauer for an ideal sail.[2]

References

[1]Zhukov, A. N., and Lebedev, V. N., "Variational Problem of Transfer Between Heliocentric Orbits by Means of Solar Sail," *Cosmic Research*, Vol. 2, No. 1, 1964, pp. 41–44.

[2]Sauer, C. G., Jr., "Optimum Solar-Sail Interplanetary Trajectories," AIAA Paper 76-792, Aug. 1976.

[3]Wood, L. J., Bauer, T. P., and Zondervan, K. P., "Comment on 'Time-Optimal Orbit Transfer Trajectory for Solar Sail Spacecraft,"' *Journal of Guidance, Control, and Dynamics*, Vol. 5, No. 2, 1982, pp. 221–224.

[4]Subba Rao, P. V., and Ramanan, R. V., "Optimum Rendezvous Transfer Between Coplanar Heliocentric Elliptic Orbits Using Solar Sail," *Journal of Guidance, Control, and Dynamics*, Vol. 15, No. 6, 1992, pp. 1507–1509.

[5]Simon, K., and Zakharov, Y., "Optimization of Interplanetary Trajectories with Solar Sail Propulsion," *Space Technology*, Vol. 16, No. 5–6, 1996, pp. 381–385.

[6]Sauer, C. G., Jr., "A Comparison of Solar Sail and Ion Drive Trajectories for a Halley's Comet Rendezvous Mission," American Astronautical Society, Paper 77-104, Sept. 1977.

[7]Cichan, T., and Melton, R. G., "Optimal Trajectories for Non-Ideal Solar Sails," American Astronautical Society, Paper 01-471, July–Aug. 2001.

[8]Colasurdo, G., and Casalino, L., "Optimal Control Law for Interplanetary Trajectories with Nonideal Solar Sail," *Journal of Spacecraft and Rockets*, Vol. 40, No. 2, 2003, pp. 260–265.

[9]McInnes, C. R., *Solar Sailing: Technology, Dynamics and Mission Applications*, Springer-Verlag, Berlin, 1999, pp. 46–53.

[10]Lawden, D. F., *Optimal Trajectories for Space Navigation*, Butterworths, London, 1963, pp. 54–68.

[11]Meeus, J., *Astronomical Algorithms*, Willmann Bell, Inc., Richmond, VA, 1991, pp. 202–204.

[12]Lewis, F. L., *Optimal Control*, Wiley, New York, 1986, pp. 235, 236.

[13]Wright, J. L., and Warmke, J. M., "Solar Sail Mission Applications," American Astronautical Society, Paper 76-808, Aug. 1976.

[14]Friedman, L., "Solar Sailing—The Concept Made Realistic," AIAA Paper 78-82, Jan. 1978.

[15]Seidelmann, P. K., *Explanatory Supplement to the Astronomical Almanac*, Univ. Science Books, Sausalito, CA, 1992, pp. 696, 697.

[16]Goldberg, D. E., *Genetic Algorithms in Search, Optimization, and Machine Learning*, Addison Wesley Longman, Reading, MA, 1989, pp. 27–86.

[17]Coleman, T. F., and Li, Y., "An Interior, Trust Region Approach for Nonlinear Minimization Subject to Bounds," *SIAM Journal on Optimization*, Vol. 6, No. 2, 1996, pp. 418–445.

[18]Lagarias, J. C., Reeds, J. A., Wright, M. H., and Wright, P. E., "Convergence Properties of the Nelder-Mead Simplex Method in Low Dimensions," *SIAM Journal of Optimization*, Vol. 9, No. 1, 1998, pp. 112–147.

[19]Dachwald, B., "Interplenatary Mission Analysis for Non-Perfectly Reflecting Solar Sailcraft Using Evolutionary Neurocontrol," American Astronautical Society, Paper 03-579, Aug. 2003.